SUPPLEMENTAL MATERIALS

METHODS

Genetic linkage analysis. In the Egyptian index family, we performed genome-wide homozygosity mapping using the Affymetrix GeneChip Human Mapping 10K Array, version 2.0 (Affymetrix), as described previously (1). GRR and PedCheck were used to verify relationships and to identify Mendelian errors. Nonparametric linkage analysis was done with MERLIN. Parametric linkage and haplotype analysis was performed using the program ALLEGRO, assuming autosomal recessive inheritance with full penetrance and a disease allele frequency of 0.0001. All data handling was performed using the graphical user interface ALOHOMORA. Graphic output of haplotypes was generated with HaploPainter. We genotyped microsatellite markers located for the two initial candidate loci on chromosome 7p15.3-p21.2 and on chromosome 15q25.3–15q26.3 (*D15S1030*, *D15S996*, *D15S963*, *D15S1514* and *D15S120*) in the Egyptian family (markers were selected from the UCSC Human Genome Browser). After exclusion of the chromosome 7 locus, mutation analysis for the candidate genes *TTC23*, *NTRK3* and *RLBP1* from the chromosome 15q25.3–15q26.3 locus was conducted by PCR-amplification and direct sequencing. Mutation screening of all known autosomal JBTS genes in G1 and G2 was likewise conducted by PCR-amplification and direct sequencing of all coding exons.

Mutation analyses. The 18 coding exons and intron-exon boundaries of *KIF7* (primers are available on request) were amplified under standard conditions and directly sequenced using Big Dye version 1.1 and an ABI 377 DNA sequencer (Applied Biosystems). Likewise, for all other JBTS genes investigated herein, the respective exons were amplified and sequenced using primers located in flanking introns and UTR sequences. Mutations were verified in ethnically matched control individuals.

Expression analysis. RT-PCR was carried out on cDNA from different tissues (retina: reversely transcribed from retinal RNA, Clontech; blood: reverse transcription from total

RNA from whole blood; cerebellum: kindly provided by B. Wirth, Institute of Human Genetics, University Hospital of Cologne; all other tissues: Human Multiple Tissue cDNA Panel I and II, Mouse Multiple Tissue cDNA Panel I, Clontech) with primers located in different exons (mouse: forward primer in exon 11, reverse primer in exon 15, product: 815 bp; human: forward primer in exon 14, reverse primer in exon 18, product: 786 bp). Samples were taken after 35 cycles of amplification.

Cell culture and transfections. HEK293T cells were transfected with plasmid DNA using a modified calcium phosphate method as described previously (2). For cilia formation, hTERT-RPE1 cells were starved for 48 hrs in the regular medium without serum. hTERT-RPE1 cells were transfected with siRNA to a final concentration of 20 nM or with plasmid DNA using oligofectamine (Invitrogen) or GeneJuice (Merck), respectively.

Antibodies. Antibodies and antisera were obtained from Sigma (anti-acetylated tubulin, anti-FLAG, anti-ß-tubulin), Serotec (anti-V5, anti-TGN46), Abnova (anti-golgin-97), Abcam (anti-pericentrin, anti-giantin), Millipore (anti-V5), Santa Cruz Biotechnology Inc. (anti-pan14-3-3), Cell Signaling Technology (anti-AKT, anti-phospho-AKT), and BD Biosciences (anti-GM130). The NPHP1 antibodies have previously been described (2, 3).

qPCR. hTERT-RPE1 cells were transfected with the indicated siRNAs using oligofectamine (20 nM final concentration). 48 hours after transfection cell were harvested in Qiazol (Qiagen) and RNA was isolated according to the manufactures protocol. After DNAse treatment (Ambion), the reverse transcription reaction was performed with ABI´s HighCapacity cDNA Kit. SYBR green qPCR was performed to evaluate mRNA levels and HPRT1 served as endogenous control. Primers had the following sequences: *KIF7*: 5' – ggcactgccagccgtgacat - 3' (fp) and 5' – tcaccccgcacagcacaaca – 3' ; *HPRT1*: 5' – tgacactggcaaaacaatgca – 3' (fp) and 5' – ggtccttttcaccagcaagct – 3'. All qPCR experiments were performed on the ABI 7900HT System and repeated four times. Error bars shown in the figures represent SEM.

Dual luciferase assay. Human *KIF7* 3'-UTR fragments were amplified from from I.M.A.G.E. cDNA clone 5724416 (Thermo Fisher, Epsom, England, GenBank accession BC040878.1) and were cloned into psiCHECK-2 (Promega) to generate *Renilla* luciferase-3'-UTR reporter constructs. Reporter assays were performe as previously describes (4). Basal expression of firefly luciferase from the same plasmid served as an internal control. HEK293T cells seeded in 96-well plates were co-transfected with plasmid (50 ng per well) and synthetic siRNA (0.25 to 2.5 pmol per well; Qiagen, Hilden, Germany) using Lipofectamine 2000. Luciferase activities were measured in a luminometer (Mithras LB940; Berthold) 24 hours after transfection. Results represent *Renilla*/firefly luciferase ratios from three independent experiments performed in triplicates. Error bars represent SEM.

Electron microscopy. For electron microscopy, cells were fixed in fresh EM-fixation (2% glutaraldehyde in 0.1 M sodium cacodylate, 0.2% picrinic acid pH 7.4) and osmicated with 1% OsO4 in 0.1 M cacodylate. Samples were dehydrated by rinsing in graded ethanol series including an uranylic acetate en bloc staining step in 70% ethanol. Before infiltration with Epon epoxy resin (Fluka, Germany) and cured for 60 h at 60°C. Thin (60 nm) cross-sections were taken on an Ultracut UCT ultramicrotome (Reichert, Heidelberg, Germany). The sections were stained with 1% aqueous uranylic acetate and lead citrate and examined with a Zeiss EM 902 electron microscope (LEO, Oberkochen, Germany).

Quantification of centrosomal duplication and cilia numbers. 24 hours after siRNA transfection of hTERT-RPE1 cells, ciliogenesis was induced by serum starvation for 48 hours as described (5). Pictures were taken with a 40x objective and centrosomes or cilia were counted using the Axiovision software (Zeiss). A minimum of 270 cells was counted for each single experiment. Co-staining with a CEP170 antibody, a marker for mother centrioles, showed complete overlap with the pericentrin signal (data not shown) suggesting that the double staining was due to centrosomal duplication rather than to centrosomal splitting. Error bars represent SEM.

References

1. Ebermann, I., Walger, M., Scholl, H.P., Charbel Issa, P., Luke, C., Nurnberg, G., Lang-Roth, R., Becker, C., Nurnberg, P., and Bolz, H.J. 2007. Truncating mutation of the DFNB59 gene causes cochlear hearing impairment and central vestibular dysfunction. *Hum Mutat* 28:571-577.
2. Benzing, T., Gerke, P., Hopker, K., Hildebrandt, F., Kim, E., and Walz, G. 2001. Nephrocystin interacts with Pyk2, p130(Cas), and tensin and triggers phosphorylation of Pyk2. *Proc Natl Acad Sci U S A* 98:9784-9789.
3. Liebau, M.C., Hopker, K., Muller, R.U., Schmedding, I., Zank, S., Schairer, B., Fabretti, F., Hohne, M., Bartram, M.P., Dafinger, C., et al. 2011. Nephrocystin-4 regulates Pyk2-induced tyrosine phosphorylation of Nephrocystin-1 to control targeting to monocilia. *J Biol Chem*.
4. Schermer, B., Ghenoiu, C., Bartram, M., Muller, R.U., Kotsis, F., Hohne, M., Kuhn, W., Rapka, M., Nitschke, R., Zentgraf, H., et al. 2006. The von Hippel-Lindau tumor suppressor protein controls ciliogenesis by orienting microtubule growth. *J Cell Biol* 175:547-554.
5. Pugacheva, E.N., Jablonski, S.A., Hartman, T.R., Henske, E.P., and Golemis, E.A. 2007. HEF1-dependent Aurora A activation induces disassembly of the primary cilium. *Cell* 129:1351-1363.

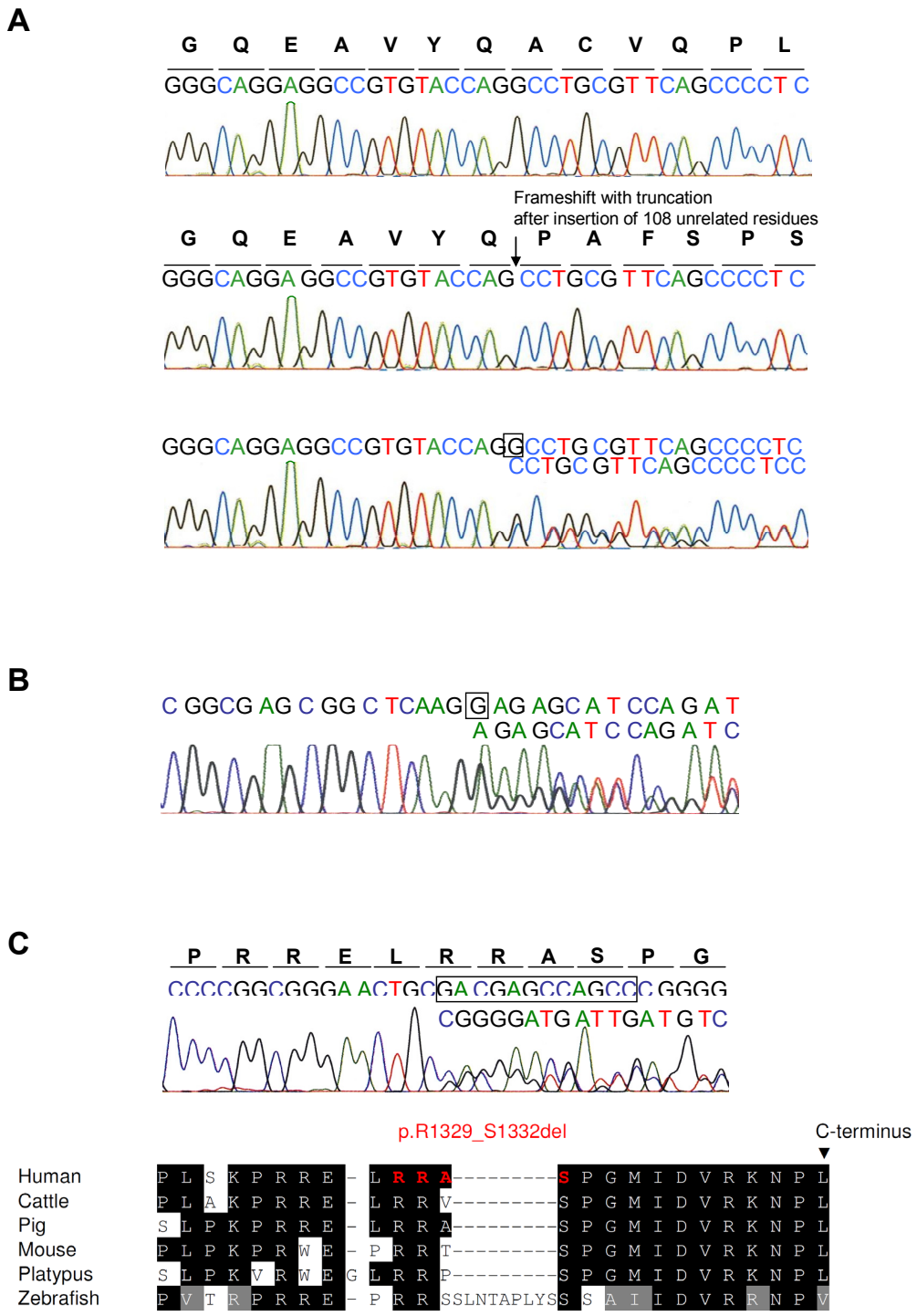

Supplemental Figure 1

Electropherograms of the *KIF7* mutations identified in this study. Deleted nucleotides are boxed. (**A**) Egyptian family. Upper panel, wild-type sequence as seen in the brothers of E2. Middle panel, homozygosity for c.217delG in patient E2. Lower panel, heterozygous mutation as found in the six carriers. (**B**) Heterozygosity for c.811delG in patient G2. (**C**) Upper panel, heterozygous in-frame deletion c.3986_3997del12 in patient G1 who is also compound heterozygous for two *TMEM67* missense mutations. Lower panel, evolutionary conservation of the KIF7 C-terminus that harbors the respective deletion of four residues (p.R1329_S1332del). Note that both arginine residues and the serine are highly conserved.

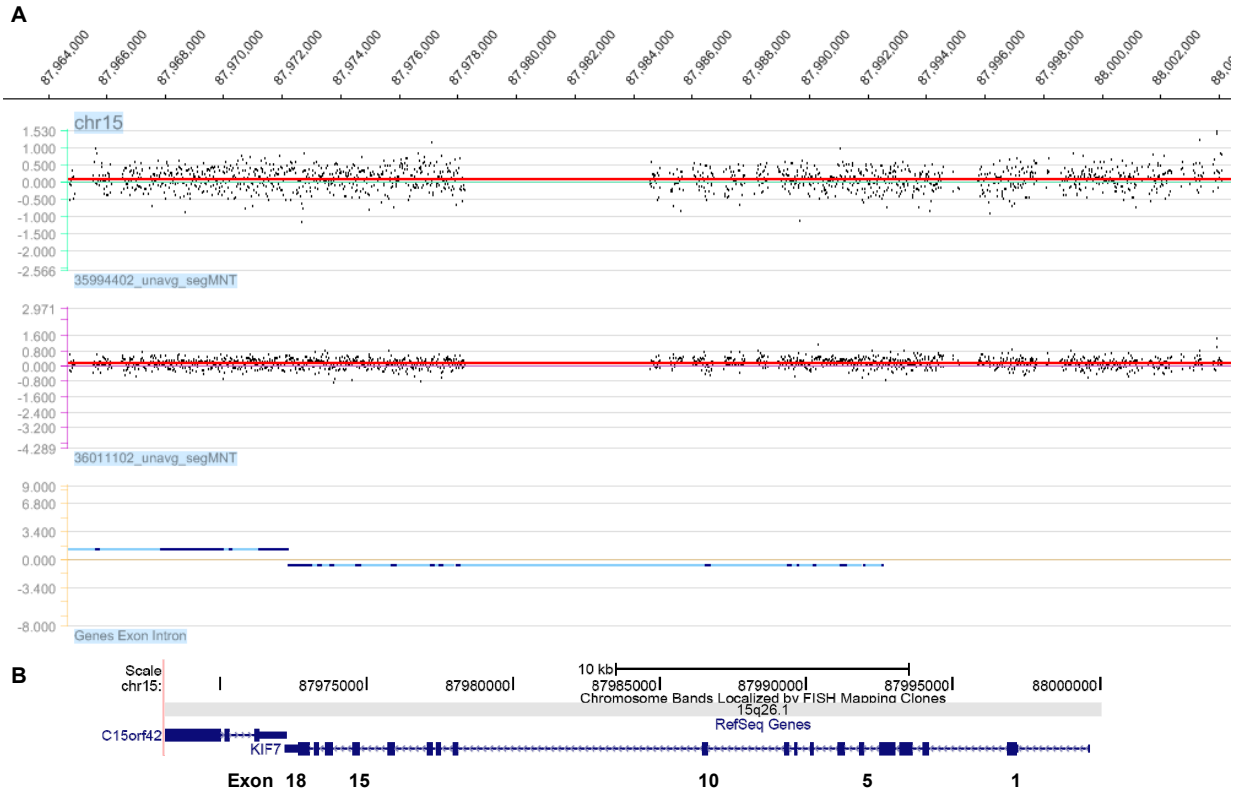

Supplemental Figure 2

Exclusion of large deletions or duplications affecting coding parts of *KIF7* in patient G2 by high-resolution array CGH using a customized NimbleGen array (black dots indicate oligonucleotide probes that densely cover the genomic *KIF7* region). Array CGH with a 6.0 Affymetrix SNP array likewise did not indicate any potentially deleterious copy number variation (not shown). (**a**) Overview of the array CGH data from the NimbleGen customized array for patients G1 (upper panel) and G2 (lower panel). (**b**) Insert from the corresponding region in the UCSC Genome Browser (hg18).

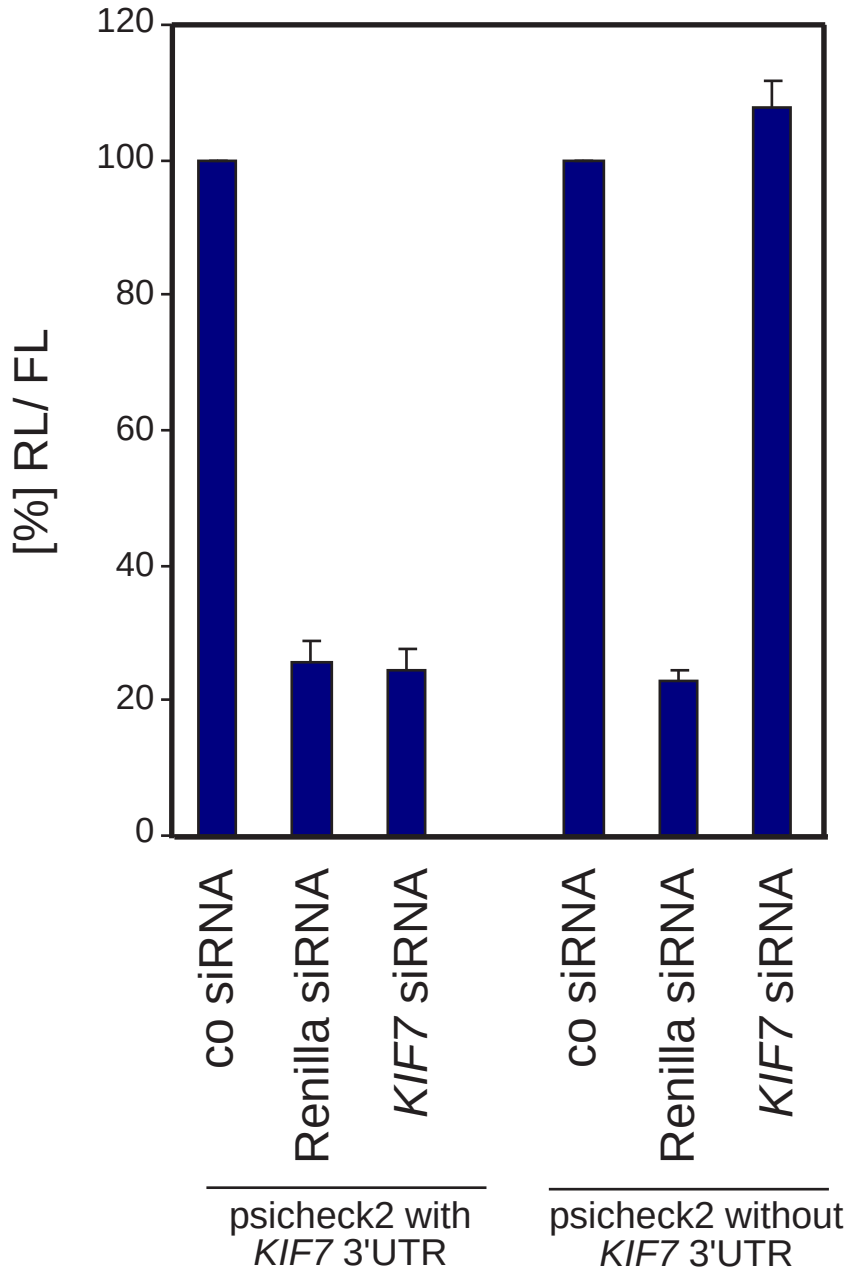

Supplemental Figure 3: Validation of siRNA directed against the 3'UTR of *KIF7* using a luciferase reporter assay. The 3'-UTR of human *KIF7* was fused with the coding sequence of *Renilla* luciferase and cloned in a bicistronic expression plasmid containing the coding sequence of firefly luciferase (psiCheck2, Promega). This plasmid was co-transfected with the particular siRNAs. Renilla luciferase activity, normalized to firefly luciferase activity, was used to assay the efficiency of the siRNA-mediated knockdown of *KIF7*. Scrambled siRNA was taken as a control. Experiments were performed in triplicate. Error bars represent SEM.

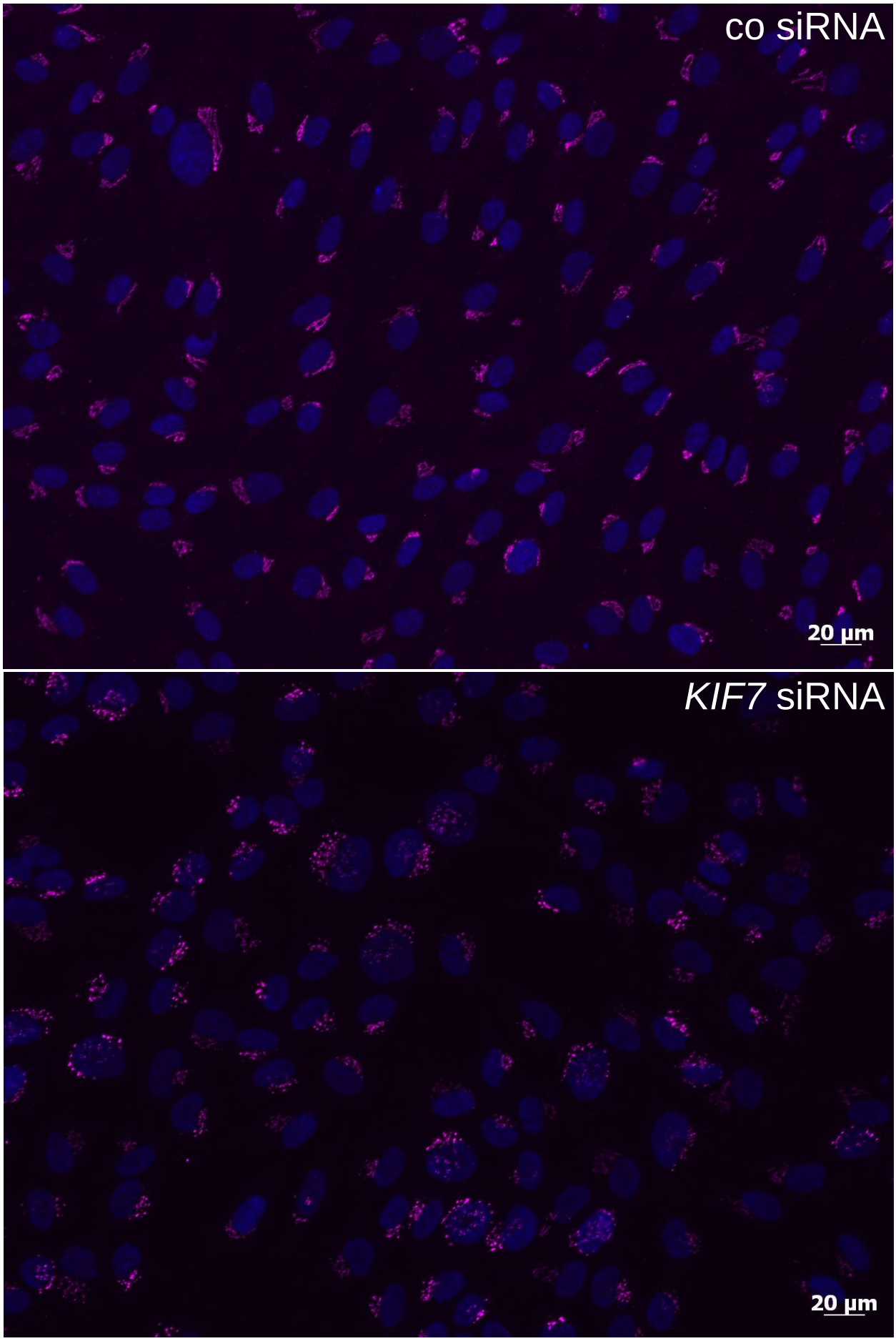

Supplemental Figure 4: Knockdown of *KIF7* induces a dispersed Golgi staining pattern. Overview of hTERT-RPE1 cells transfected with *KIF7* siRNA or control siRNA, stained for the Golgi marker golgin-97 (close-up views of these experiments are shown in Fig. 2A).

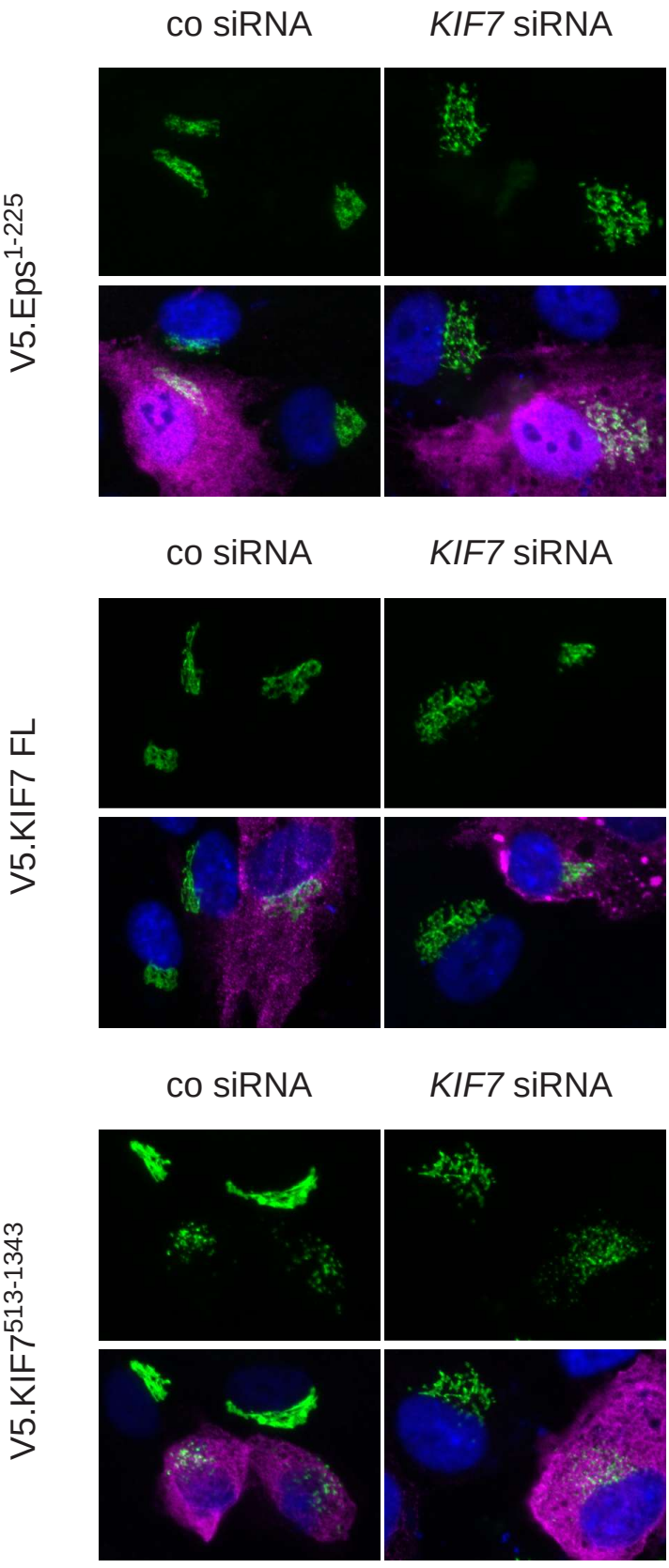

Supplemental Figure 5: The observed Golgi phenotype is specific for the loss of *KIF7* function. hTERT-RPE1 cells were transfected with either siRNA against the 3'-UTR of *KIF7* (right) or control siRNAs (left). Co-transfected plasmids encoded either for a control protein (V5.EPS$^{1-225}$; upper panel), V5.KIF7 FL (middle panel) or a truncated form of V5.KIF7 (513-1343; lower panel). Cells were fixed and co-stained with the Golgi marker GM-130 (green) and an anti-V5 antibody (magenta) for the detection of the transfected proteins. Co-expression of KIF7 FL, but not of EPS $^{1-225}$ or of KIF7 $^{513-1343}$ was able to rescue the *KIF7* siRNA phenotype. Expression of the KIF7 $^{513-1343}$, a truncation lacking the predicted motor domain causes a similar phenotype in control siRNA-transfected cells as seen in *KIF7* knockdown cells (lower panel).

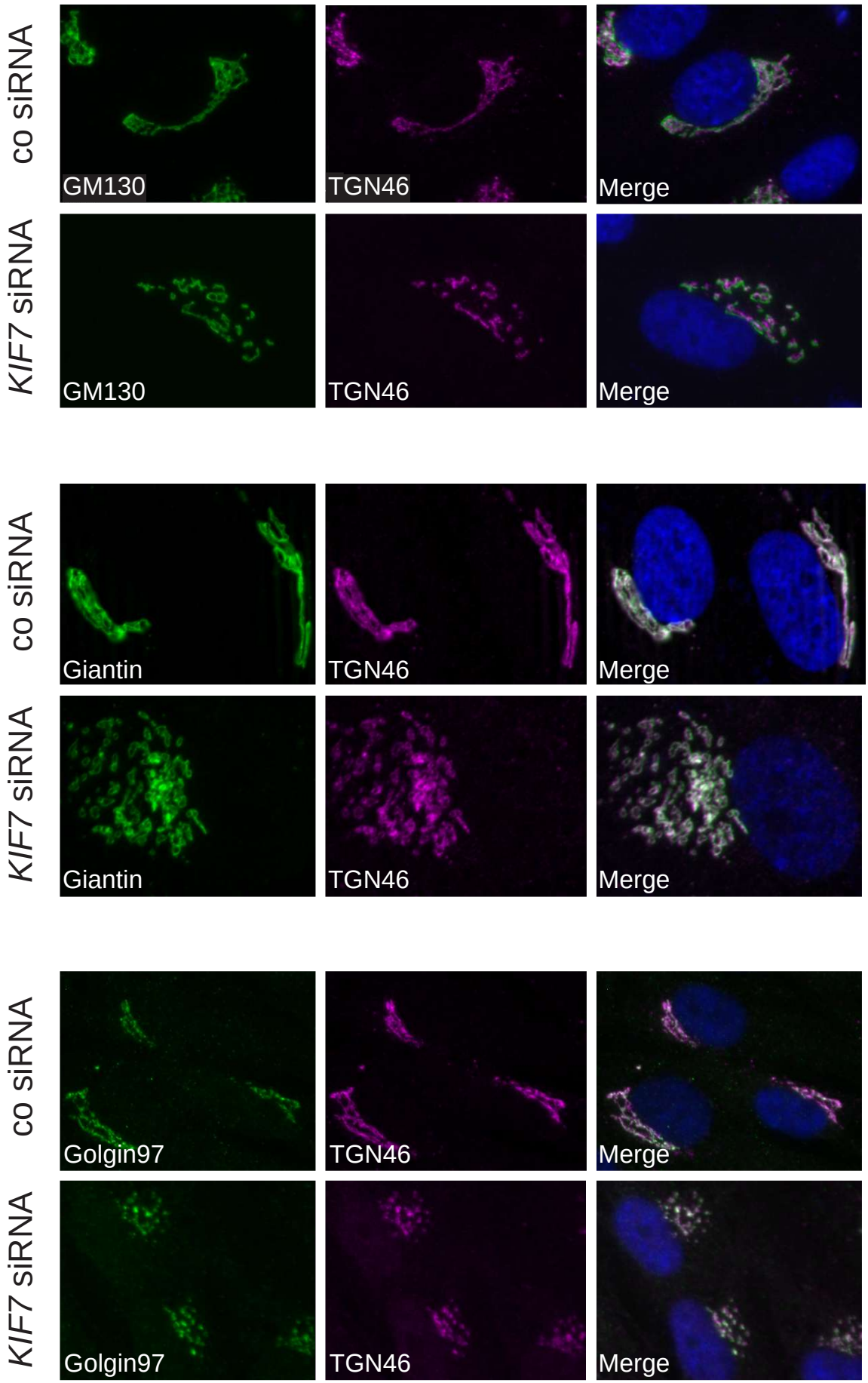

Supplemental Figure 6: Knockdown of *KIF7* affects all compartments of the Golgi apparatus. hTERT-RPE1 cells were transfected with either siRNA against *KIF7* (lower row) or control siRNAs (upper row in each panel). The results obtained for the Golgi marker golgin-97 were confirmed using markers for cis- (GM130), cis-/medial- (giantin) and trans- (TGN46) Golgi-networks. This revealed that all three Golgi networks are affected by knocking down *KIF7*.

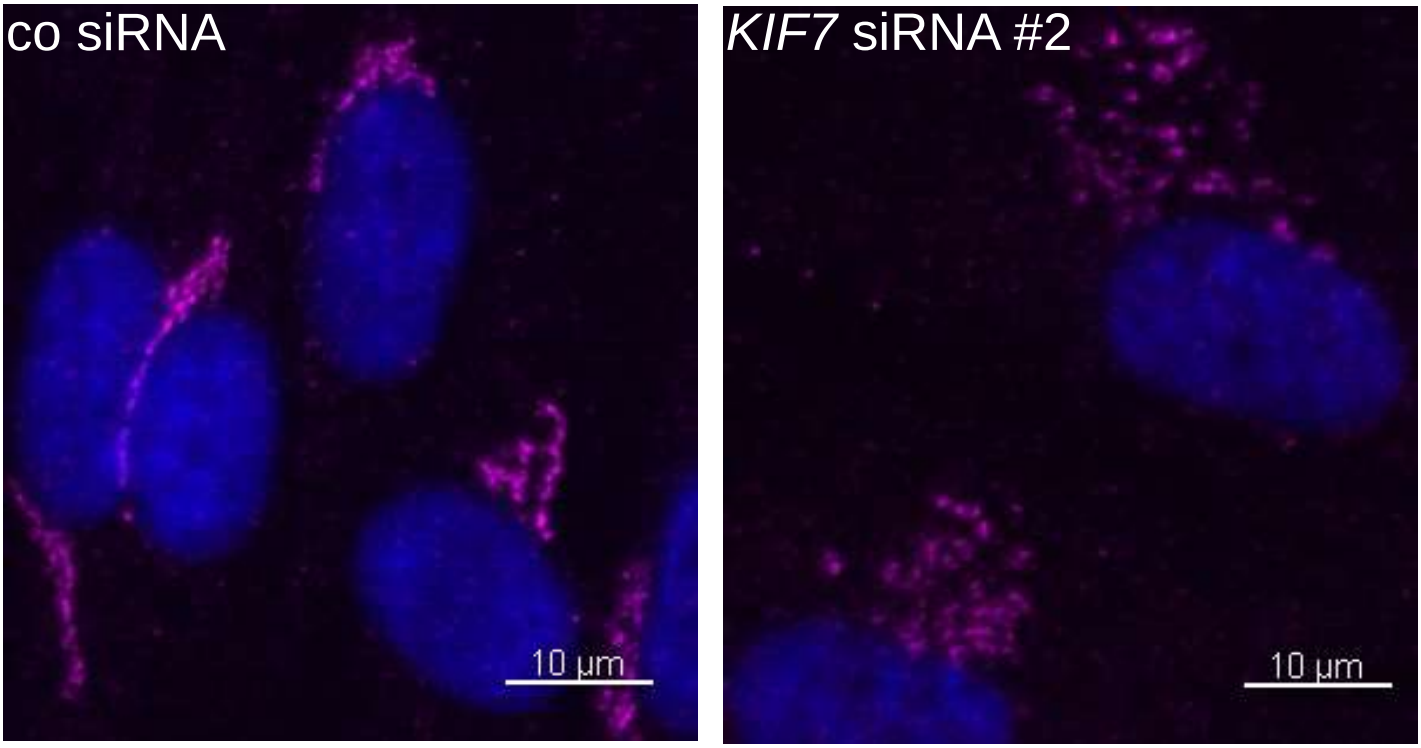

Supplemental Figure 7: The effect of *KIF7* knockdown on the Golgi apparatus was confirmed using an independent siRNA directed against the coding sequence of *KIF7*. Cells were transfected with either this siRNA or control siRNA and stained for the Golgi marker golgin-97.

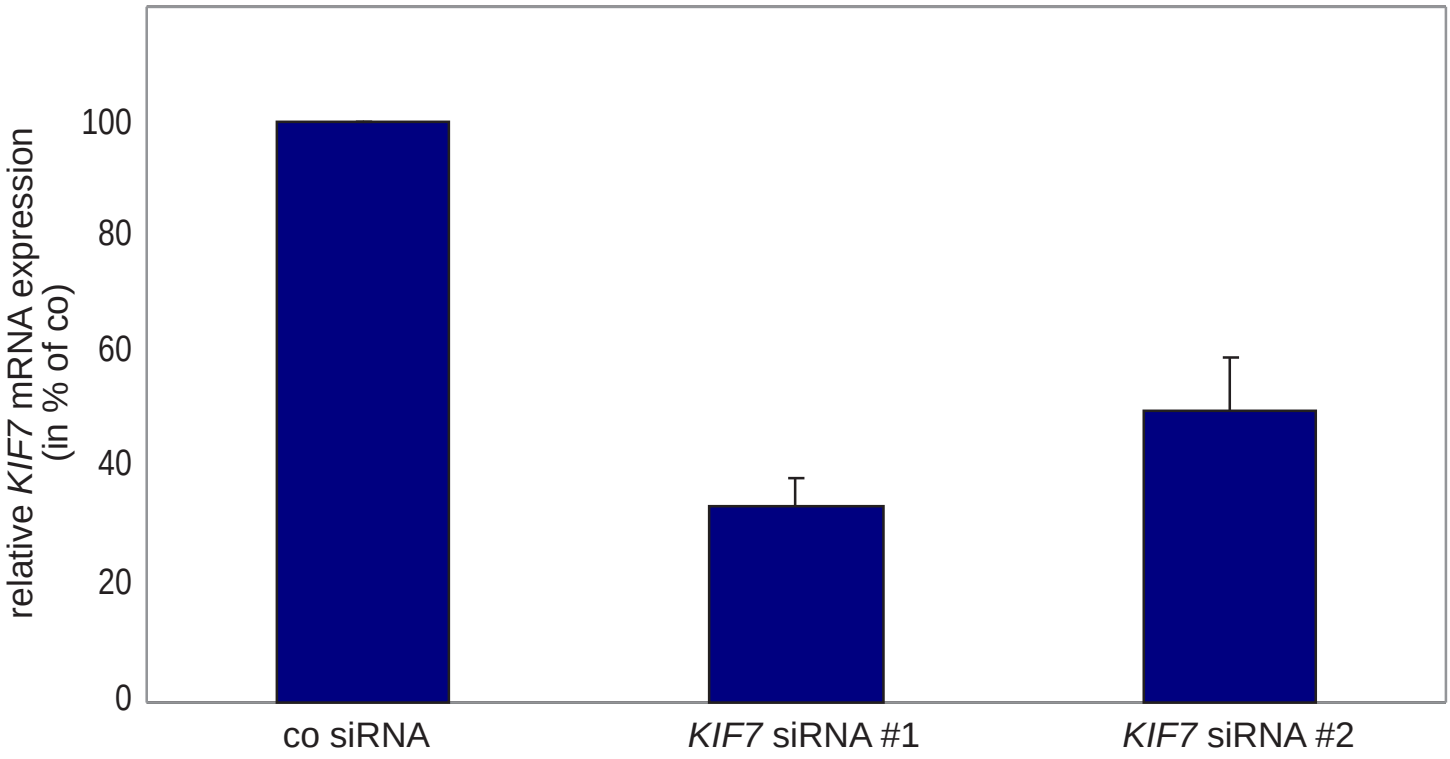

Supplemental Figure 8: Validation of siRNA-induced *KIF7* knockdown. hTERT-RPE1 cells were transfected with either control siRNA or siRNA directed against *KIF7* (#1 against 3'-UTR; #2 against coding sequence) used in this study. The specific knockdown of *KIF7* was quantified by qPCR (n=4).

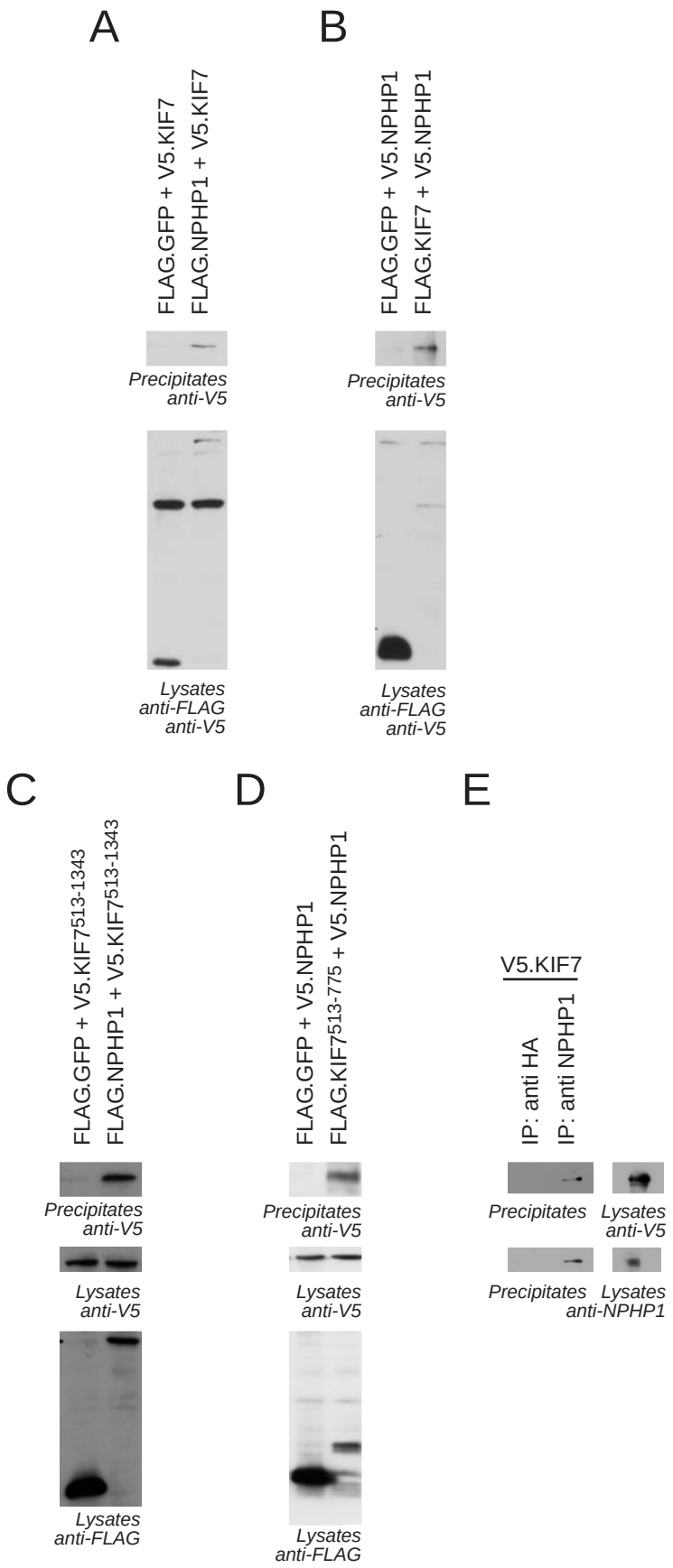

Supplemental Figure 9: Interaction of KIF7 with the known JBTS protein nephrocystin-1 (NPHP1). (A, B) KIF7 and NPHP1 full-length proteins co-precipitate. (C) A C-terminal truncation of KIF7 starting at amino acid residue 513 specifically co-precipitates with NPHP1. (D) A short truncation of KIF7 containing amino acid residues 513-775 is capable to precipitate NPHP1. (E) Semiendogenous immunoprecipitation. Endogenous NPHP1 precipitates overexpressed KIF7.

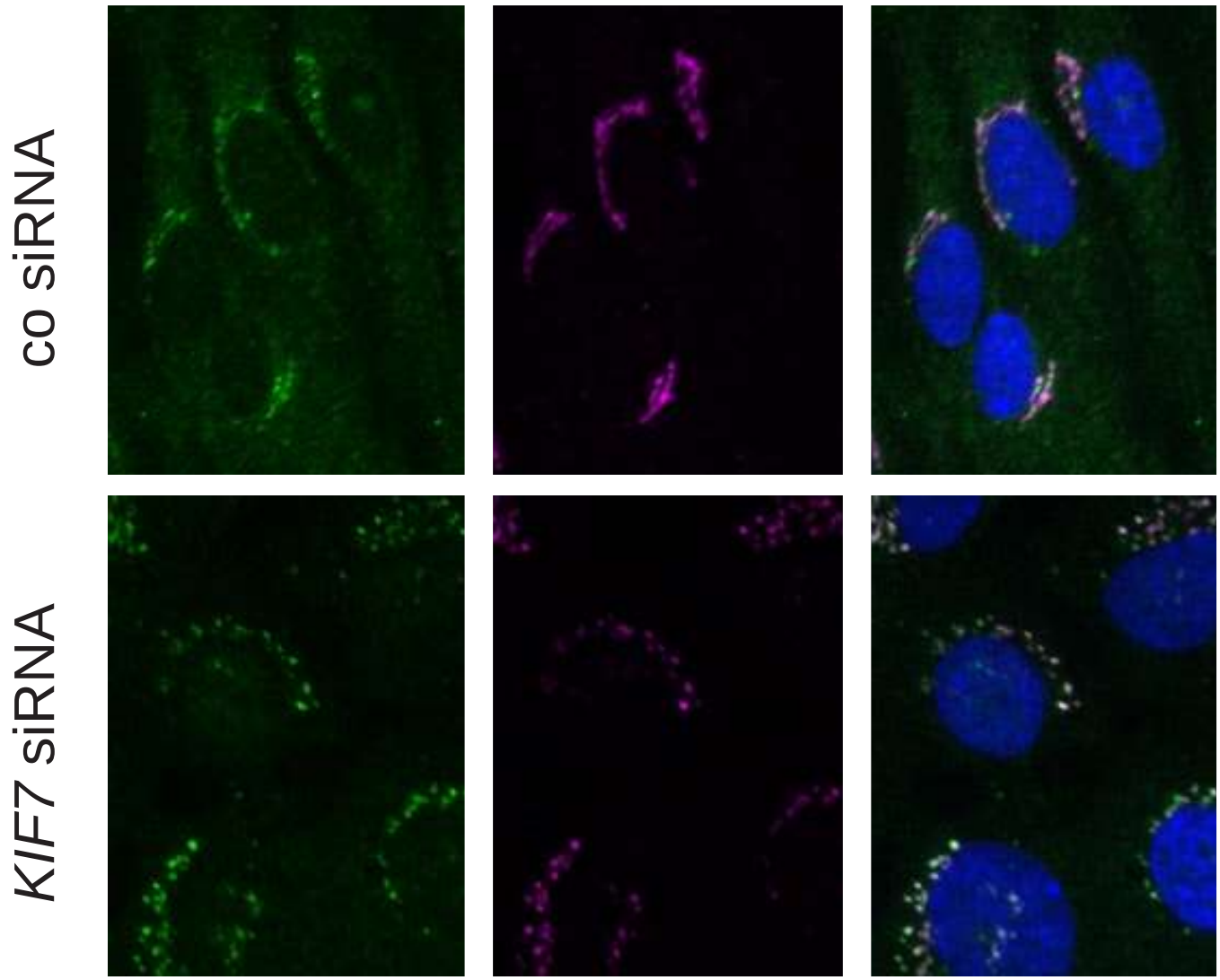

Supplemental Figure 10: *KIF7* knockdown affects NPHP1 localization. hTERT-RPE1 cells were transfected with control siRNA or *KIF7* siRNA and co-stained for NPHP1 (green) and the Golgi marker golgin-97 (magenta). *KIF7* knockdown cells showed a NPHP1 re-distribution according to the severe Golgi phenotype.

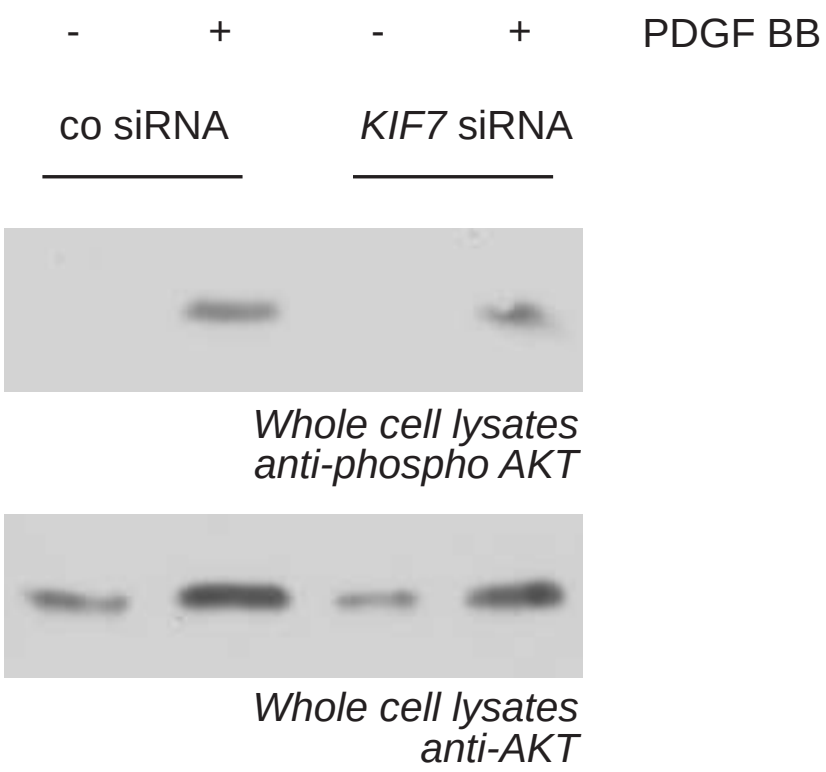

Supplemental Figure 11: *KIF7* knockdown does not affect phosphatidylinositol phosphate (PIP) signaling. hTERT-RPE1 cells were transfected with control siRNA or *KIF7* siRNA. Cells were starved for 16 hours and stimulated with recombinant PDGF BB (50 ng/ml, 10 min). Western blot analysis of whole cell lysates did not reveal a difference in phosphorylation of AKT at serine-473.

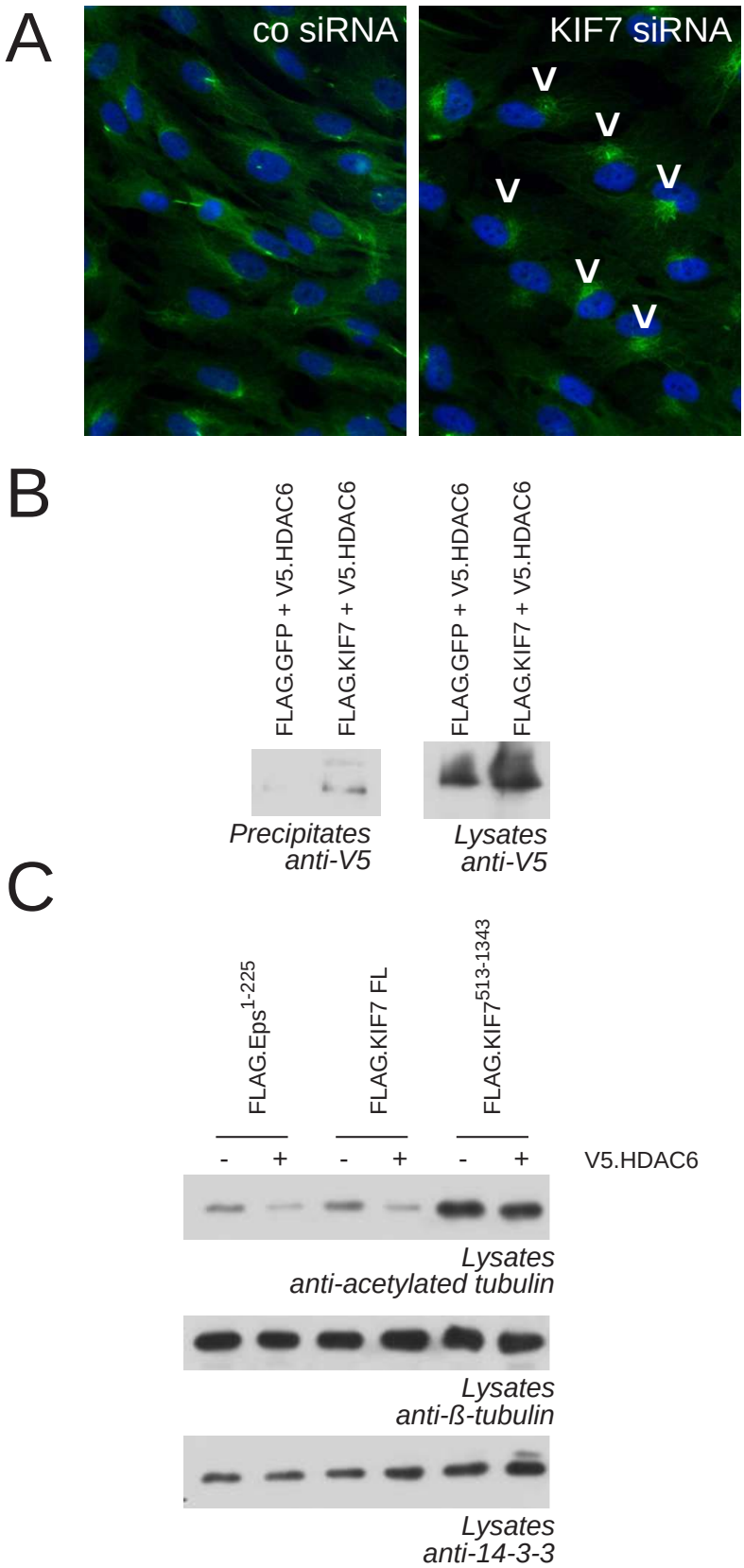

Supplemental Figure 12: KIF7 modulates HDAC6-induced deacetylation of microtubules. (A) Knockdown of *KIF7* stabilizes acetylated microtubuli on ice. hTERT-RPE1 cells were transfected with control siRNA or *KIF7* siRNA. To induce microtubular de-polymerisation, cells were incubated on ice for 30 minutes. The cells were subsequently stained for acetylated tubulin. (B) KIF7 interacts with HDAC6. HDAC6 specifically co-precipitates with KIF7 but not with a control protein. (C) KIF7 modulates HDAC6 function. Expression of KIF7 $^{513-1343}$, but not of KIF7 FL, leads to a HDAC6-resistant hyperacetylation of tubulin in HEK293T cells.